A Novel Green's Function Analysis of Wave Scattering by an Infinite Grating using Complex Images Technique

[1]H. Alaeian and [2]R. Faraji-Dana

Center of Excellence on Applied Electromagnetic Systems,
School of Electrical & Computer Engineering, University of Tehran, P.O. Box 14395-515, Tehran, Iran
[1]h.alaian@ece.ut.ac.ir, [2]reza@ut.ac.ir

Abstract **–** A new method, based on the complex images technique is presented for solving the electromagnetic scattering from the infinite metallic and dielectric gratings. The main idea of this method lies in representing the infinite summation of the structure period Green's functions in terms of finite summations of complex images. The method of moments (MoM) is then employed to find the current distribution, reflection and transmission coefficients of the gratings. The validity of the presented method is shown through various examples for different grating geometries and incident wave polarizations. Fast convergence, simple formulations and flexibility of the method in analyzing different structures are the main advantages of the proposed method.

Keywords: Integral equation, grating, Green's function, complex image.

I. INTRODUCTION

Theoretical studies of electromagnetic scattering from periodic metallic or dielectric structures or gratings go back to more than a hundred years ago [1, 2]. Since then various analytical or numerical techniques have been developed to formulate the electromagnetic scattering from the periodic scatterers [3, 4].

The interesting feature of these structures as frequency and polarization selective devices and their extra degree of freedom in controlling the scattered fields, have made them an important choice in design and fabrication of various devices especially at microwave and optical frequencies. In fact they have been used extensively in the fabrication of devices such as filters, waveguides, couplers, sensors, antenna substrates and reflectors [5, 6].

In recent years the emergence of photonic bandgap devices in discrete periodic dielectric and metallic structures and their potentials in realizing narrow-band filters, high-quality resonators, linear waveguides and mirrors have attracted much attention toward the topic of periodic structures. Beside photonics, plasmonic phenomena dealing with periodic metallic structures in optical frequencies further improved this topic. The observation of enhanced transmission phenomena in subwavelength perforated metallic screens has directed lots of studies to the investigation of transmittance and reflectance behavior of the metallic gratings in those devices [7, 8].

A one-dimensional periodic array of cylindrical objects made of metal or dielectric is a typical geometry of periodic structures. The frequency response of the array is determined by the scattering characteristics of each cylinder and the multiple scattering under the presence of the periodic scatterers. A two-dimensional photonic bandgap structure can be obtained with multilayered one-dimensional arrays. The multiple interaction of the scattered space harmonics from these layers modifies the electromagnetic properties of the final structure [9]. Various frequency responses can be obtained by using different types of scatterers and arranging them in different geometries. During the past decade, a vast amount of investigation on the electromagnetic scattering by layered periodic arrays of cylindrical objects has been done. In these investigations various techniques such as mode matching method, homogenization method, Fourier modal method, finite difference method and time domain techniques have been applied to the periodic structures [9-17]. Integral equation methods are among the most accurate and flexible semi-analytical approaches that have been used in analyzing such structures [18]. Efficient computation of the slowly convergent series of periodic Green's functions encountered in these methods is still the main challenge of their applications in this domain.

In this paper, we will present an accurate integral equation method for dealing with a two-dimensional electromagnetic scattering from periodic arrays of cylindrical objects based on the complex images Green's function, for the first time. The approach is quite general with the capability to be applied on various configurations of periodic arrays of two-dimensional metallic or dielectric cylindrical objects. In the proposed method the periodic Green's function has been efficiently approximated with a finite series of complex images and a closed form can be obtained through this approximation. This approximated Green's function has

been used afterward in the analysis of the one-dimensional periodic cylindrical objects. The reflectance and transmittance behavior of metallic and dielectric gratings with circular and rectangular cross-sectioned rods for different polarizations have been computed and compared as a representation of the method versatility.

This paper is organized as follows. In section II, the complex images representation of the Green's function for one-dimensional periodic structures is developed. Section III is devoted to the MoM formulation of the problem based on the developed complex images Green's function. As E and H-modes are two independent solutions of the 2D case, the formulation has been done for these two cases, separately. The diffraction properties of a general polarization can be obtained through its decomposition to these two fundamental modes.

In section IV numerical results will be presented. At first the validity of the complex images Green's function is shown through an example. Then the grating simulation results will be presented showing the behavior of different gratings against various polarizations. The validity of these results has been investigated by checking the energy balance and edge conditions. Concluding remarks with be given in section V.

II. COMPLEX IMAGES REPRESENTATION OF A 1-D PERIODIC GREEN'S FUNCTION

According to Floquet-Bloch theorem Eigen modes in a periodic lattice can be expressed as $G(\vec{r})\exp(-j\vec{k}.\vec{r})$ where G is the distribution in a unit cell and $\vec{k}$ is the lattice wavevector [19]. This simply means that the propagation of a mode in a periodic lattice leads to a phase change without any variations in the form of its distribution. Using this concept, it is quite straight forward to show that the Green's function of a one-dimensional periodic structure, as shown in Fig.1 can be expressed as,

$$G^{per}(\vec{r}\,|\,\vec{r}\,') = \sum_{m=-\infty}^{\infty} G(\vec{r}\,|\,x'+md, y', z')\, e^{-jmdk_x} \quad (1)$$

where G is the Green's function of a source of the array and d is the period of the lattice (Fig. 1). As the gratings are composed of two-dimensional cylindrical objects, one-dimensional array of line sources should be considered here. Therefore $G(r,r')$ can be written as,

$$G = \frac{1}{4j} H_0^{(2)}\left(k_0\sqrt{(x-x'-md)^2+(y-y')^2}\right). \quad (2)$$

The series in equation (1) converges very slowly especially when the observation point is far from the field point. It is also known that applying Poisson's transform to that series leads to its corresponding modal series which suffers from slow convergence for near fields. In order to accelerate the convergence of these kind of series different methods such as Kummer's transform, Ewald transform and Shank's transform have been proposed in the literature [20, 21]. Although these methods can be successfully applied to the periodic Green's functions in the form of equation (1), it must be kept in mind that these Green's functions are used in the kernel of the integral equations. Therefore the employed integral equation methods will suffer from numerical deficiency as the Green's functions would have no closed form representation. In the complex images representation developed below however, the periodic Green's function of equation (1) is given in a closed form which is valid for all the sources and field points. This will bring numerical efficiency to the relevant integral equation techniques.

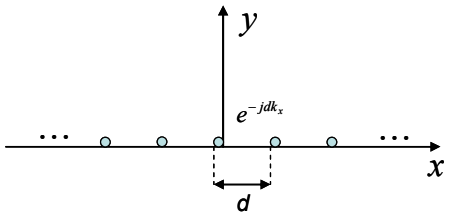

Fig. 1. One-dimensional array of line sources.

In order to derive the complex images representation of equation (1) while $G(r,r')$ has been replaced with equation (2), we can use the following identity,

$$\frac{1}{4j} H_0^{(2)}\left(k_0\sqrt{(x-md)^2+y^2}\right) = \frac{1}{2\pi}\int_{-\infty}^{\infty} \frac{e^{-j\beta_x|x-md|}}{j2\beta_x} e^{-jk_y y}\, dk_y \quad (3)$$

where $\beta_x = \sqrt{k_0^2 - k_y^2}$.

By substituting equation (3) in equation (1) and changing the order of summation and integration operators, a geometric series will be obtained. For field points in a unit cell i.e. $0<x<d$ ($x'=0$ is assumed) after some simple manipulations the following equation can be obtained,

$$G^{per}(\vec{r}\,|\,\vec{r}\,') = \frac{1}{2\pi}\int_{-\infty}^{\infty} \frac{e^{-jk_y y}}{j2\beta_x}\left[\frac{e^{-j\beta_x x}}{1-e^{j(k_x-\beta_x)d}}\, dk_y + \frac{e^{-j\beta_x|x-d|}}{1-e^{-j(k_x+\beta_x)d}}\, dk_y\right]. \quad (4)$$

As the name of complex images technique implies the main goal is to preserve the form of the original sources and find an approximation that its terms resemble the ones in the first series [22]. Obviously this aim can be fulfilled if the fractions in the kernel of inverse Fourier

Transform integral of equation (4) can be approximated by a finite series of exponential. That is,

$$\frac{e^{-j\beta_x x}}{1-e^{j(k_x-\beta_x)d}} = e^{-j\beta_x x} + \frac{e^{j(k_x-\beta_x)d}}{1-e^{j(k_x-\beta_x)d}}\, e^{-j\beta_x x} = e^{-j\beta_x x} + \sum_{m=1}^{M_1} a_m e^{-j(x+jb_m)\beta_x} \quad (5a)$$

and

$$\frac{e^{-j\beta_x|x-d|}}{1-e^{-j(k_x+\beta_x)d}} = e^{-j\beta_x|x-d|} + \frac{e^{-j(k_x+\beta_x)d}}{1-e^{-j(k_x+\beta_x)d}}\, e^{-j\beta_x|x-d|} = e^{-j\beta_x|x-d|} + \sum_{m=1}^{M_2} c_m e^{-j(|x-d|+jd_m)\beta_x} . \quad (5b)$$

Prony's method [22], GPOF [23] or least square methods can be used to realize these approximations accurately. The approximation path of Fig. 2 in the β_x plane has been found to be appropriate to perform the above approximations. In this path T_0 is determined according to the relative distance between field and source points [22]. It may be mentioned that the existence of poles which may occur near the approximation path (Fig. 2) can deteriorate the above mentioned approximation. In that case one can extract the poles from the approximating function and include its effects manually [22].

Substituting the above approximations in equation (4) and using the identity equation (3) leads to,

$$\begin{aligned} G^{per}(r,r') = {} & \frac{1}{4j}H_0^{(2)}(k_0\sqrt{x^2+y^2}) + \\ & e^{-jdk_x}\frac{1}{4j}H_0^{(2)}(k_0\sqrt{(x-d)^2+y^2}) + \\ & \sum_{m=1}^{M_1} a_m \frac{1}{4j}H_0^{(2)}(k_0\sqrt{(x+jb_m)^2+y^2}) + \\ & \sum_{m=1}^{M_2} c_m e^{-jdk_x}\frac{1}{4j}H_0^{(2)}(k_0\sqrt{(|x-d|+jd_m)^2+y^2}) . \end{aligned} \quad (6)$$

This completes the derivation of complex images representation of the periodic Green's function of equation (1). It can be seen that the first two terms in equation (6) correspond to the two of sources in the array that have the most effects on the field points located in a unit cell. The presence of these two terms in the final representation guarantees satisfactory results for the near fields especially in the vicinity of the boundaries. The two finite summations in equation (6) correspond to the complex images which have the same forms as real sources in the array except that they are located in complex positions and have complex values. They are more important when the field point is located away from the boundaries within a unit cell. It is clear that equation (6) offers a closed form representation of the Green's functions in terms of two finite summations; so the issue of convergence for infinite series does not exist anymore. It is clear that the same procedure can be applied to an array of point sources. Moreover it can be easily extended to 2-D periodic Green's functions of line sources, and to the 2-D and 3-D periodic Green's functions of point sources.

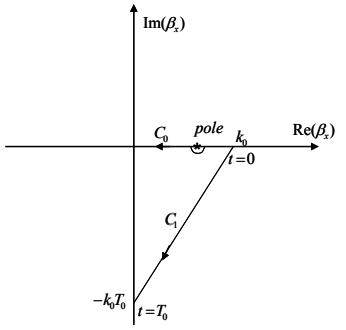

Fig. 2. The approximation path in the β_x plane.

Examination of the accuracy of the developed complex images Green's function will be deferred until section V.

III. MOM FORMULATION OF THE PROBLEM

Figure 3 shows a grating of typical cylindrical objects studied in this paper illuminated by a plane wave with wavevector $\bar{k}$. Since there is no variation along the z-axis, TE and TM polarizations can exist independently.

In TM polarization (H_x, H_y, E_z) are the only existing components of the EM fields. For PEC rods in the array, by applying the proper boundary condition on the rod located in the unit cell, the following electric field integral equation (EFIE) determines the current flowing on the rod.

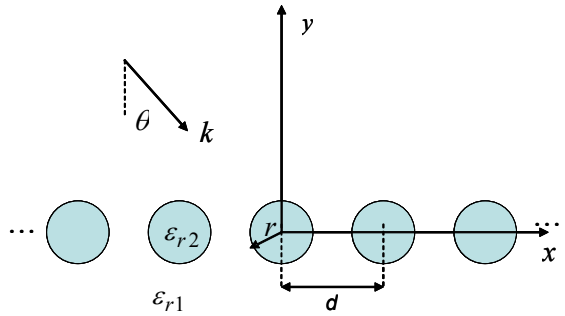

Fig. 3. Cross section of a grating of typical cylindrical objects.

$$E_z^{inc}(l) = j\omega\mu_0 \oint_{body} G^{per}(l,l')J_z(l')dl' . \quad (7)$$

In TE polarization (E_x, E_y, H_z) are the only existing components of the EM fields. Considering the same PEC rods and formulating the problem for magnetic field after applying the proper boundary condition on the rod, the following magnetic field integral equation (MFIE) gives the current distribution.

$$J_l(l) = H_z^{inc}(l) + \oint_{body} \frac{\partial G^{per}(l,l')}{\partial n'} J_l(l')dl' . \quad (8)$$

In the above integral equations G^{per} is given by equation (6) while l represents the transverse coordinate on a rod [24].

For a grating made of dielectric rods instead of PEC (Fig. 3), one can derive the integral equations by using the equivalent surface electric and magnetic currents and boundary integral equations (BIE). The equivalent surface currents are given by,

$$\begin{aligned} \vec{J}_s(l) &= \alpha \hat{n} \times \vec{H}_t(l) \\ \vec{M}_s(l) &= -\alpha \hat{n} \times \vec{E}_t(l) \end{aligned} . \quad (9)$$

Where subscript t represents the total field on the boundary of the rod and α is a factor equal to 1 and -1 for exterior and interior problems, respectively. Using these equivalent currents the following equations can be written for exterior and interior regions in TM polarization, respectively,

$$\begin{aligned} &\vec{E}^{inc}(l) + \vec{E}^{sca}(l) = 0 \quad l \in interior\ region \\ &\vec{E}^{sca}(l) = 0 \quad l \in exterior\ region . \end{aligned} \quad (10)$$

Similarly the above equations can be written for H in a TE polarized illumination.

To solve for the unknown current distribution in the above integral equations, the method of moments has been employed by using pulse basis functions and applying the point matching technique [24]. When the current distribution has been determined all the diffraction characteristics of the grating can be obtained using the scattered fields.

Because of the periodic nature of the structure the reflected and transmitted electromagnetic waves contain infinite diffraction orders. The parallel component of the diffraction orders can be obtained from the following formula,

$$k_{\parallel} = k_x + \frac{2m\pi}{d} = k_0 \sin\theta + \frac{2m\pi}{d} \quad m \in Z . \quad (11)$$

The reflectance and transmittance of a grating order have been defined as the ratio of the power carried in that order to the incident power. For a diffracted plane wave to carry energy away from the grating, the following condition must be satisfied,

$$k_0 \geq | k_0 \sin\theta + \frac{2m\pi}{d} | \quad . \quad (12)$$

In the above relation m is an algebraic integer representing the order of diffraction. The above formula explicitly shows that the number of propagating waves that carry energy away from the grating depends on the incident angle and the normalized frequency as well. The power transmitted to each diffraction order can be controlled by the geometry of the grating and the type of elements composing the array. Using multilayer gratings with various elements one can control the diffraction characteristics of the gratings as well.

Applying different optimization algorithms on the structure it can be optimized to carry power in a determined diffraction order or to obtain a desired frequency response.

In the next section the simulation results of plane wave scattering by different gratings in both polarizations will be presented.

IV. NUMERICAL RESULTS

In this section, first the numerical accuracy of the developed complex images Green's function is examined by using an example. In this example d=4, λ=5 and k_x=0 are assumed in the array of line sources (Fig. 1). Table 1 gives the values of exponential coefficients in the complex images representation (5) for M_1=M_2=5 found through the GPOF algorithm when the path truncation parameter T_0=15 is assumed (Fig. 2).

Table 1. Exponential coefficients for d=4, λ=5 and k_x=0.

a_m	b_m
$(-0.1416-j0.2625)\times10^{-10}$	17.7235-j17.9114
$(-0.1226-+j0.9336)\times10^{-4}$	7.6704-j13.2827
0.0554-0.0106	2.0320-j9.5251
0.7973-j0.6096	-0.04528-j7.6087
1.00425+j0.00564	0.00123-j4.0030

Figure 4 shows the magnitude of the error between the exact spectral function (5a) and its finite summation approximation found through the GPOF technique. The error has been computed along the approximation path of Fig. 2 for different number of exponentials used in the summation. It can be seen that for just 3 terms in the exponential summation an accurate approximation of the spectral function is achieved almost along the whole path.

This demonstrated the efficiency of the proposed approximation.

Figure 5 compares the magnitude and phase of $G^{pre}(r,r')$ found by complex images representation of equation (6) with the values of the Green's function in the form of infinite images and modal series accelerated with the Shanks' transform. It can be seen that the results obtained by the complex images method are in excellent agreements with those obtained from image and modal series. Also it can be observed that the complex images results show the singularity of the source near the boundary while the modal series has difficulty in showing this behavior as its convergence deteriorates in the near fields.

Figure 6 shows the convergence of the approximate complex images Green's function versus number of terms in the summation by evaluating the errors between the results obtained form the infinite modal series and the finite summation of complex images. It is clear that even for small number of terms, i.e., for M=6 negligible errors occur in the proposed complex images representation.

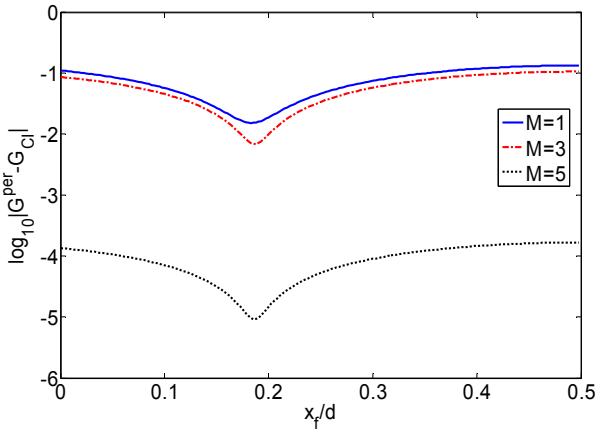

Fig. 6. The magnitude of error at different field points in complex images Green's function for different exponential terms.

The proposed approach has been used in the analysis of various metallic and dielectric gratings. All gratings have been investigated for their reflectance behavior in subwavelength regime where d/λ<1. In order to study the frequency and polarization selectivity of these structures their responses for different normalized frequencies and polarizations have been obtained. Since, as a filter, the sensitivity of the response to the incident angle is an important factor, this factor has been studied by considering the arrays in a fixed normalized frequency for various incident angles. Finally the effect of the shape on the responses has been studied with comparison of the results of the circular cross sectioned cylinders with square ones. The reflected and transmitted EM fields in each order have been evaluated on a constant line above and below the grating.

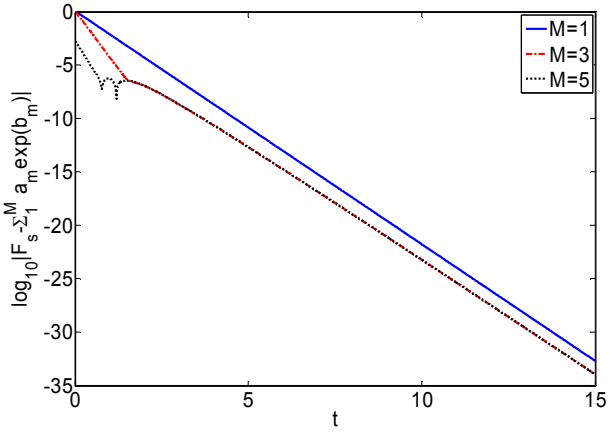

Fig. 4. The magnitude of error between the spectral function and its corresponding finite summation approximation for different number of exponential terms.

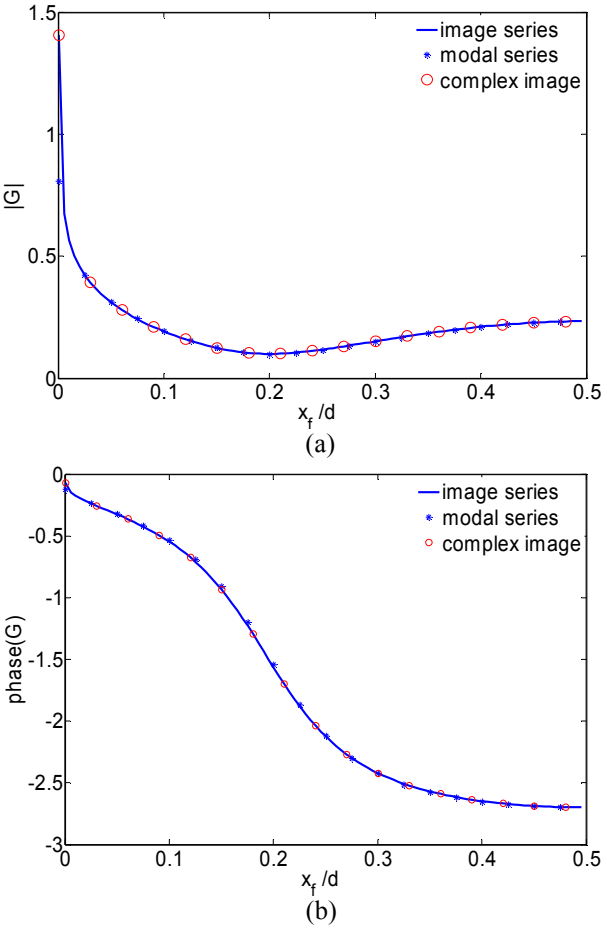

Fig. 5. (a) Magnitude, (b) phase of the periodic Green's function of 1-D line sources with d=4, λ=5 and k_x=0 for field points on the x-axis.

The first example (Fig. 7) compares the zeroth order reflection coefficient, R_0, of a metallic grating composed of PEC rods with $r = 0.15d$ with one of a dielectric grating with $r = 0.3d$ and $\varepsilon_r = 2$ for TM polarization. In this case, since the zeroth order is the only propagating component that carries power away from the grating, the figure contains that diffraction order only. Good agreements can be observed between these results and those reported in [25]. In the above figure there is a resonance frequency in the dielectric case while PEC array does not show this behavior.

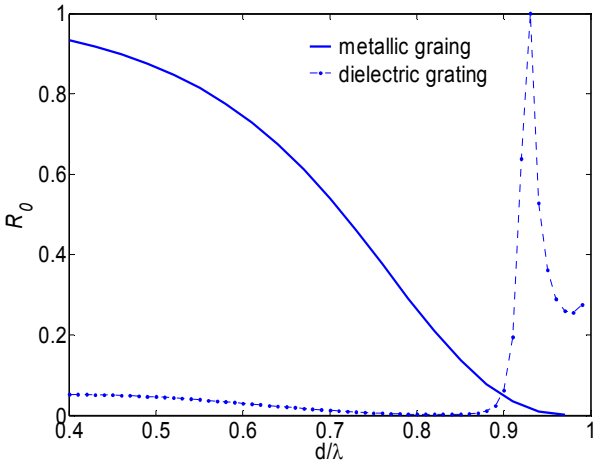

Fig. 7. R_0 versus normalized frequency for gratings composed of PEC rods with r=0.15d and dielectric rods with r=0.3d.

Figure 8 shows the frequency response of a grating composed of PEC rods with r/λ=0.08 located in a medium with ε_{r1}=2.33 when a TM polarized plane wave illuminates the array at θ=45°. Variations of the reflection coefficients R_0, R_{-1}, R_{-2} are given versus the normalized frequency $NF = d/\lambda$.

In this case the metallic grating reflects all the power in a wide range of frequencies and behaves as a reflector. At *NF=0.39* the -1st diffraction order gains the power and decreases the power carried by the zeroth order. At *NF=0.77* the -2nd order carries power as well. Figure 9 shows the response of the same array at *NF=0.5* when the TM polarized incident plane wave illuminates the grating at different angles.

The last example compares the effect of the rods geometry on the diffraction characteristics of the grating. Figure 10 compares the frequency response of the zeroth order reflection coefficient of two metallic gratings, one made of rods with circular cross-section (with r/λ=0.08) and the other made of rods with square cross-section (with a/λ=0.16, where *a* denotes the square side). Both gratings are located in a medium with ε_{r1}=2.33 and are illuminated with a TE-polarized plane wave at θ=45°.

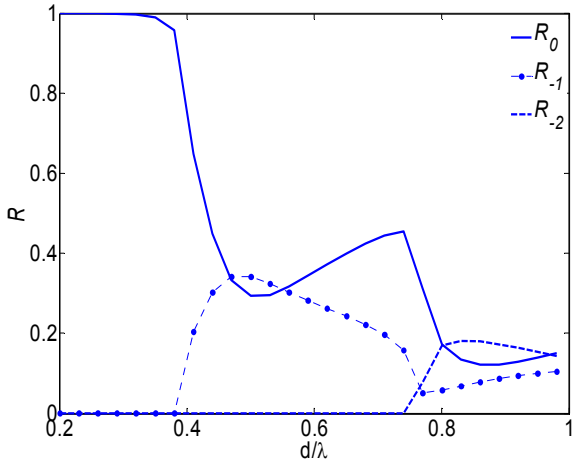

Fig. 8. R_0, R_{-1} and R_{-2} versus normalized frequency for a metallic grating with ε_{r1}=2.33, r=0.08λ and θ=45° for TM polarization.

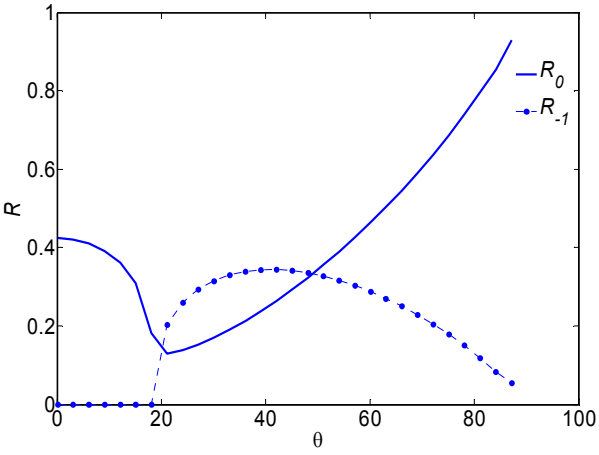

Fig. 9. R_0 and R_{-1} vs. incident angle for a metallic grating with ε_{r1}=2.33, r=0.08λ and NF=0.5 for TM polarization.

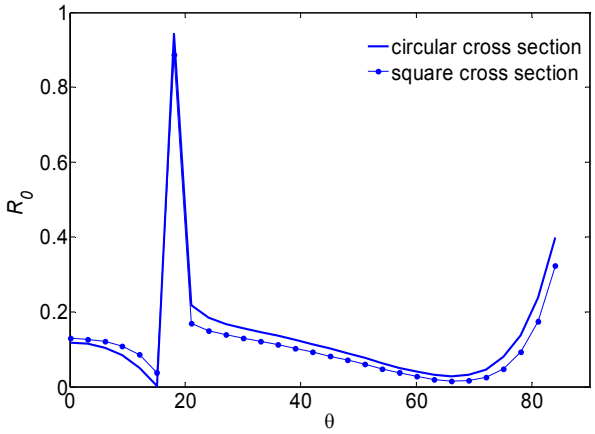

Fig. 10. Comparison of R_0 versus incident angle for two metallic gratings made of rods with circular cross-section with r=0.08λ, and square cross-section with a/λ=0.16 at NF=0.5 for TE polarization.

Comparing these results with those presented in Fig. 9 reveals that the response of a metallic grating varies drastically as the polarization changes. While most of the power is reflected by the grating in TM polarization, in the TE case considerable amount of power is transmitted except for an anomalous increase observed at $\theta=18^{o}$ angle. Also it can be observed that the rods geometry affects the diffraction characteristics of the grating significantly.

V. CONCLUSION

In this paper a novel complex images representation of the free-space periodic Green's function has been presented. Using this closed form representation, fast and accurate computation of the Green's function is possible for all the field points. Moreover each term in this representation has the same form as the sources forming the periodic array, i.e. a line source for 2-D sources and a point source for 3-D sources. This will facilitate the application of integral equation techniques for analyzing the periodic structures under study significantly.

Using the developed complex images Green's functions in the integral equations, 1-D periodic structures made of PEC or dielectric rods have been investigated and their diffraction characteristics in TE and TM polarizations have been studied.

Although single-row 1-D periodic arrays were considered here, the method can be easily applied to multi-row gratings with different periods and various elements in each row.

ACKNOWLEDGMENT

This work was partially supported by Iran Telecommunication Research Center (ITRC) through a research Grant.

REFERENCES

[1] H. Lamb, "On the reflection and transmission of electric waves by metallic grating," *Proc. London Math. Soc.* vol. 29, no. 1, pp. 523-545, 1898.

[2] L. Rayleigh, "On the dynamical theory of grating," *Proc. R. Soc. (London)*, Ser. A, vol. 79, pp. 399-416, 1907.

[3] V. Twersky, "On scattering of waves by the infinite grating of circular cylinders," *IRE Trans. Antennas Propagat.*, vol. 10, pp. 737-765, Nov. 1962.

[4] M. J. Lockyear, A. P. Hibbins, K. R. White, and J. R. Sambles, "One-way diffraction grating," *Phys. Rev. E* 74, 056611, 2006.

[5] J. M. Lourtioz, A. de Lustrac, F. gadot, S. Rowson, A. Chelnokov, T. Brillat, A. Ammouche, J. Danglot, O. Vanbesien, and D. Lippens, "Toward controllable photonic crystals for centimeter- and millimeter-wave devices," *J. Lightw. Technol.,* vol. 17, no. 11, pp. 2025-2031, Nov. 1999.

[6] A. Scherer, T. Doll, E. Yablonovitch, H. O. Everitt, and J. A. Higgins, "Special section on electromagnetic crystal structures, design, synthesis, and applications," *J. Lightw. Technol.,* vol. 17, no. 11, pp. 1928-2207, 1999.

[7] B. Pradarutti, C. Rau, G. Torosyan, and R. Beigang, "Plasmonic response in a one-dimensional periodic structure of metallic rods," *Appl. Phys. Lett.* 87, 24105, 2005.

[8] K. F. Tsang, L. Mo, and Z. B. Ye, "Analysis of millimeter wave scattering by the infinite plane metallic grating using PCG-FFT technique," *International J. Infrared Millimeter waves*, vol. 24, no. 6, pp. 1005-1022, Jun. 2003.

[9] K. Yasumoto, H. Toyama, and T. Kushta, "Accurate analysis of two-dimensional electromagnetic scattering from multilayered periodic arrays of circular cylinders using lattice sums technique," *IEEE Trans. Antennas Propagat.*, vol. 52, no. 10, pp. 2603-2611, Oct. 2004.

[10] E. Popov and B. Bozhkov, "Differential method applied for photonic crystals," *Appl. Opt.,* vol. 39, no. 27, pp. 4926-4932, 2000.

[11] M. Koshibe, Y. Tsuji, and M. Hikari, "Time-domain beam propagation methods and its application to photonic crystal circuits," *J. Lightw. Technol.*, vol. 18, no. 1, Jan. 2000.

[12] S. F. Halfert and R. Pregla, "Efficient analysis of periodic structures," *J. Lightw. Technol.*, vol. 16, no. 9, Sep. 1998.

[13] H. Jia and K. Yasumoto, "S-Matrix solution of electromagnetic scattering from periodic arrays of metallic cylinders with arbitrary cross section," *IEEE Antennas Wireless Propagat. Lett.*, vol. 3, pp. 41-44, Jan. 2004.

[14] M. Ohki, T. Kurihara, and S. Kozaki, "Analysis of electromagnetic wave diffraction from a metallic Fourier grating by using the T-matrix method," *JEMWA*, vol. 11, pp. 1257-1272, 1997.

[15] M. Ohki, K. Sato, M. Matsumoto, and S. Kozaki, "T-Matrix analysis of electromagnetic wave diffraction form a dielectric coated Fourier grating," *PIER,* vol. 53, pp. 91-108, 2005.

[16] H. A. Kalhor, "EM scattering by an array of perfectly conducting strips by a physical optics approximation," *IEEE Trans. Antennas Propagat.*, vol. 28, no. 2, pp. 277-278, Mar. 1980.

[17] N. P. K. Cotter, T. W. Preist, and J. R. sambles, "Scattering-matrix approach to multilayer diffraction," *J. Opt. Soc. Am. A*, vol. 12, pp. 1097-1103, 1995.

[18] R. Petit, *Electromagnetic Theory of Gratings*, Springer-verlag, New York 1980.

[19] R. Collin, *Field Theory of Guided Waves.* McGraw-Hill, New York, USA, 2nd ed., 1991.
[20] S. Singh, W. F. Richards, J. R. Zinecker, and D. R. Wilton, "Accelerating the Convergence of Series Representing the Free Space Periodic Green's function", *IEEE Trans. Antennas Propagat.*, vol. 38, no. 12, pp. 1958-1962, Dec. 1990.
[21] R. Lampe, P. Klock, and P. Mayes, "Integral Transforms Useful for the Accelerated Summation of Periodic Free-Space Green's Function," *IEEE Trans. Microw. Theory Tech.*, vol. 33, no. 8, pp. 734-736, Aug. 1985.
[22] Y. L. Chow, J. J. Yang, D. G. Fang, and G. E. Howard, "A closed-form spatial Green's function for the thick microstrip substrate," *IEEE Trans. Microw. Theory Tech.*, vol. 39, no. 3, pp. 588- 592, Mar. 1991.
[23] Y. Hua and T. K. Sarkar, "Generalized Pencil-of-Function method for extracting poles of an EM system from its transient response," *IEEE Trans. Antennas Propagat.*, vol. 37, pp. 229-234, 1989.
[24] R. F. Harrington, *Field Computation by Moment Methods.* New York: IEEE Press, 2nd Ed., 1993.
[25] T. Kushta and K. Yasumoto, "Electromagnetic scattering from Periodic Arrays of Two Circular Cylinders per Unit Cell," *PIER*, vol. 29, pp.69-85, 2000.

Hadiseh Alaeian was born in 1984 in Tehran, Iran. She received the B.Sc. and M.Sc. degrees in electrical engineering from the University of Tehran, Iran, in 2004 and 2006, respectively. She is currently a research assistant in the antenna laboratory of the school of Electrical and Computer Engineering at the University of Tehran. Her major areas of interest are electromagnetic bandgap structures and their modeling, meta-materials and THz devices.

Reza Faraji-Dana received the B.Sc. degree (with honors) from the University of Tehran, Tehran, Iran, in 1986 and the M.A.Sc. and Ph.D. degrees from the University of Waterloo, Waterloo, ON, Canada, in 1989 and 1993, respectively, all in electrical engineering. He was a Postdoctoral Fellow with the University of Waterloo for one year. In 1994, he joined the School of Electrical and Computer Engineering, University of Tehran, where he is currently a Professor. He has been engaged in several academic and executive responsibilities, among which was his deanship of the Faculty of Engineering for more than four years, up until summer 2002, when he was elected as the University President by the university council. He was the President of the University of Tehran until December 2005. He is the author of several technical papers published in reputable international journals and refereed conference proceedings.

Prof. Faraji-Dana has been the Chairman of the IEEE-Iran Section since March 2007. He received the Institution of Electrical Engineers Marconi Premium Award in 1995.